

1 A descriptive marker gene approach to single-cell pseudotime 2 inference

3 Kieran R Campbell^{1,2,5,*} and Christopher Yau^{2,3,4}

4 ¹Department of Physiology, Anatomy and Genetics, University of Oxford, UK

5 ²Wellcome Trust Centre for Human Genetics, University of Oxford, UK

6 ³Department of Statistics, University of Oxford, UK

7 ⁴Centre for Computational Biology, University of Birmingham, UK

8 ⁵Current address: Department of Statistics, University of British Columbia, Vancouver BC,
9 Canada

10 *kieran.campbell@stat.ubc.ca

11 November 2, 2017

12 Abstract

13 Pseudotime estimation from single-cell gene expression allows the recovery of temporal information from
14 otherwise static profiles of individual cells. This pseudotemporal information can be used to characterise
15 transient events in temporally evolving biological systems. Conventional algorithms typically emphasise an
16 unsupervised transcriptome-wide approach and use retrospective analysis to evaluate the behaviour of in-
17 dividual genes. Here we introduce an orthogonal approach termed “Ouija” that learns pseudotimes from a
18 small set of marker genes that might ordinarily be used to retrospectively confirm the accuracy of unsup-
19 versed pseudotime algorithms. Crucially, we model these genes in terms of switch-like or transient behaviour
20 along the trajectory, allowing us to understand why the pseudotimes have been inferred and learn informa-
21 tive parameters about the behaviour of each gene. Since each gene is associated with a switch or peak
22 time the genes are effectively ordered along with the cells, allowing each part of the trajectory to be un-
23 derstood in terms of the behaviour of certain genes. In the following we introduce our model and demon-
24 strate that in many instances a small panel of marker genes can recover pseudotimes that are consistent
25 with those obtained using the entire transcriptome. Furthermore, we show that our method can detect dif-
26 ferences in the regulation timings between two genes and identify “metastable” states - discrete cell types
27 along the continuous trajectories - that recapitulate known cell types. Ouija therefore provides a powerful
28 complimentary approach to existing whole transcriptome based pseudotime estimation methods. An open
29 source implementation is available at <http://www.github.com/kieranrcampbell/ouija> as an R package and
30 at <http://www.github.com/kieranrcampbell/ouijaflow> as a Python/TensorFlow package.

31 Introduction

32 The advent of high-throughput single-cell technologies has revolutionised single-cell biology by allowing dense
33 molecular profiling for studies involving 100-10,000s of cells [1–6]. The increased availability of single-cell data
34 has driven the development of novel analytical methods specifically tailored to single cell properties [7, 8]. The
35 difficulties in conducting genuine time-series experiments at the single-cell level has led to the development
36 of computational techniques known as *pseudotime ordering* algorithms that extract temporal information from
37 snapshot molecular profiles of individual cells. These algorithms exploit studies in which the captured cells
38 behave asynchronously and therefore each is at a different stage of some underlying temporal biological pro-
39 cess such as cell differentiation. In sufficient numbers, it is possible to infer an ordering of the cellular profiles
40 that correlates with actual temporal dynamics and these approaches have promoted insights into a number of
41 time-evolving biological systems [9–19].

42 A predominant feature of current pseudotime algorithms is that they emphasise an “unsupervised” ap-
43 proach. The high-dimensional molecular profiles for each cell are projected on to a reduced dimensional
44 space by using a (non)linear transformation of the molecular features. In this reduced dimensional space, it
45 is hoped that any temporal variation is sufficiently strong to cause the cells to align against a trajectory along

46 which pseudotime can be measured. This approach is therefore subject to a number of analysis choices
47 including gene selection, dimensionality reduction technique, and cell ordering algorithm, all of which could
48 lead to considerable variation in the pseudotime estimates obtained. In order to verify that any specific set of
49 pseudotime estimates are biologically plausible, it is typical for investigators to retrospectively examine specific
50 marker genes or proteins to confirm that the predicted (pseudo)temporal behaviour matches *a priori* beliefs.
51 An iterative “semi-supervised” process maybe therefore be required to concentrate pseudotime algorithms on
52 behaviours that are both consistent with the measured data and compliant with a limited amount of known
53 gene behaviour.

54 In this paper we present an orthogonal approach implemented within a Bayesian latent variable statistical
55 framework called ‘Ouija’ that learns pseudotimes from small panels of putative or known marker genes (Figure
56 1A). Our model focuses on switch-like and transient expression behaviour along pseudotime trajectories, ex-
57 plicitly modelling when a gene turns on or off along a trajectory or at which point its expression peaks. Crucially,
58 this allows the pseudotime inference procedure to be understood in terms of descriptive gene regulation events
59 along the trajectory (Figure 1B). As each gene is associated with a particular switch or peak time, it allows us to
60 order the genes along the trajectory as well as the cells and discover which parts of the trajectory are governed
61 by the behaviour of which genes. For example, if the pseudotimes for a set of differentiating cells run from 0
62 (stem cell like) to 1 (differentiated) and only two genes have switch times less than 0.25 then a researcher
63 would conclude that the beginning of differentiation is regulated by those two genes. We further formulate a
64 Bayesian hypothesis test as to whether a given gene is regulated before another along the pseudotemporal
65 trajectory (Figure 1C) for all pairwise combinations of genes. Furthermore, by using such a probabilistic model
66 we can identify discrete cell types or “metastable states” along continuous developmental trajectories (Figure
67 1D) that correspond to known cell types.

68 In the following we introduce our model and demonstrate that it allows pseudotimes equivalent to those in-
69 ferred using transcriptome-wide models to be learned from only small panel of marker genes. We demonstrate
70 that our model is robust to departures from the prior specification of gene behaviour and that it can identify
71 metastable states along continuous pseudotemporal trajectories consistent with experimentally validated cell
72 types. Finally, we show through simulations that informative Bayesian priors on behaviour parameters may
73 increase the accuracy of pseudotime orderings. An open source implementation of our model is available
74 at <http://www.github.com/kieranrcampbell/ouija> as an R package and as a Python/TensorFlow package
75 <http://www.github.com/kieranrcampbell/ouijaflow>.

76 Results

77 Pseudotime inference from small marker gene panels

78 The transcriptomes of both single cells and bulk samples exhibit remarkable correlations across genes and
79 transcripts. Such concerted regulation of expression is thought to be due to pathway-dependent transcription
80 [21, 22] and is necessary for the field of network inference from gene expression data [23]. An example of
81 such transcriptome wide correlations can be seen in Figure 2A for the Trapnell et al. [12] dataset, where
82 hierarchical clustering of gene-gene correlations reveals a block-diagonal structure of genes organised into
83 distinct transcriptional pathways. These large correlations across genes imply an intrinsic low-dimensionality
84 of the data meaning it can be efficiently compressed, using techniques such as principal components analysis
85 (PCA). For the Trapnell et al. [12] dataset thousands of genes across the transcriptome exhibit high correlations
86 with the first two principal components (Supplementary Figure 1A) which explain around 20% of the variance
87 (Supplementary Figure 1B).

88 This redundancy of expression is often exploited by statistical models of single-cell RNA-seq data. He-
89 imberg et al. [24] use the intrinsic low-dimensionality of the data to reconstruct transcriptome-wide gene
90 expression from ultra-shallow read depths. Cleary et al. [25] apply compressed sensing techniques from the
91 field of signal processing to demonstrate that low-dimensional random projections can efficiently reconstruct
92 high-dimensional gene expression profiles. Rather than explicitly reduce the dimensionality of the data, Mc-
93 Curdy et al. [26] propose a column subset selection procedure whereby a small number of genes are chosen
94 to represent the full transcriptome and demonstrate that this allows clustering of the cells in a similar manner
95 to using the full transcriptomes.

96 The compressibility of transcriptome data is likewise exploited by many single-cell pseudotime inference
97 algorithms via initial dimensionality reduction steps. For example, Monocle [12] begins by reducing the expres-
98 sion data down to 2 dimensions using independent component analysis, while both TSCAN [18] and Waterfall
99 [16] apply PCA to reduce the data down to 2 dimensions. The implication behind such an approach is that there
100 is sufficient information in just two dimensions of the data via a linear projection to learn “transcriptome-wide”
101 pseudotime and that the majority of expression is redundant given the low-dimensional projection. Nonlinear di-
102 mensionality reduction techniques underpin alternative pseudotime approaches such as diffusion components

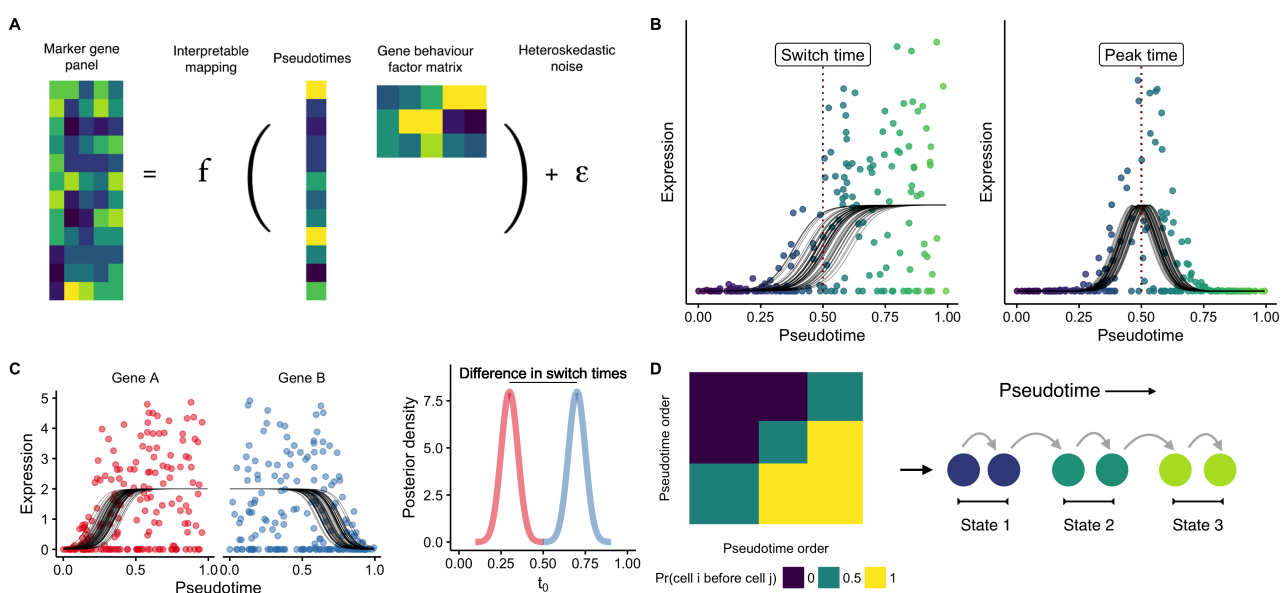


Figure 1: Learning single-cell pseudotimes with parametric models. **A** Ouija infers pseudotimes using Bayesian nonlinear factor analysis by decomposing the input gene expression matrix through a parametric mapping function (sigmoidal or transient). The latent variables become the pseudotimes of the cells while the factor loading matrix is informative of different types of gene behaviour. A heteroskedastic dispersed noise model with dropout is used to accurately model scRNA-seq data. **B** Each gene's expression over pseudotime is modelled either as a sigmoidal shape (capturing both linear and switch-like behaviour) or through a Gaussian shape (capturing transient expression patterns). These models include several interpretable parameters including the pseudotime at which the gene is switched on and the pseudotime at which a gene peaks. **C** The posterior distributions over the switch and peak times can be inferred leading to a Bayesian statistical test of whether the regulation of a given gene occurs before another in the pseudotemporal trajectory. **D** Ouija can identify discrete cell types that exist along continuous trajectories by clustering the matrix formed by considering the empirical probability one cell is before another in pseudotime.

in DPT [27] or reverse graph embedding in Monocle 2 [8].

In Ouija, we exploit the high gene-gene correlations by modelling a small number of *marker* genes that are representative of the whole transcriptome. Such an approach is advantageous as by modelling the data directly rather than a reduced-dimension representation we can understand the pseudotimes for each cell in terms of the behaviour of genes through time rather than abstract notions of manifolds embedded in high-dimensional space. This takes the form of a nonlinear factor analysis model, departing from previous models that have relied upon linear factor analysis [28, 29] by introducing sigmoidal nonlinearities (successfully applied previously to single-cell data [30, 31]) and through transient expression functions.

We then turn to the question of how to choose the small number of marker genes in order to fit the pseudotimes. In single-cell pseudotime studies, the cells under examination undergo a known biological process such as differentiation or cell cycle. Importantly, key marker genes associated with these processes are usually known *a priori* by investigators. These marker genes act as positive controls whose behaviour is used post-hoc to confirm the validity of the transcriptome-wide pseudotime fit. For example, in [12] the cells undergo myogenesis and the validity of the pseudotime is confirmed by upregulation of markers of myoblast differentiation such as *MYH3*, *MEF2C*, and *MYOG*, along with down-regulation of markers of actively proliferating cells such as *CDK1* and *ID1*. In [16], the cells undergo neurogenesis and the validity of the transcriptome-wide fit is confirmed via the upregulation of several markers of neural stem cells including *Gfap* and *Sox2*. Further, in [32] the authors tabulate the marker genes they expect to be involved in the process along with their expected behaviour along the differentiation trajectory. Given both the widespread *a priori* knowledge of such markers and their requirement to validate transcriptome-wide pseudotime fits, we therefore propose to derive pseudotimes directly from such markers using our proposed model below.

We first sought to test whether our model applied to small panels of marker genes could accurately recapitulate the transcriptome-wide pseudotimes inferred by popular pseudotime methods. We applied Monocle 2, DPT, and TSCAN to five publicly available single-cell RNA-seq datasets [12, 16, 33–35] using the 500 most variable genes as input (the default in packages such as Scater [36] for PCA representations). For each dataset, we then inferred pseudotimes using Ouija based only on a small number of marker genes reported in each paper (ranging from 5 to 12), and compared the Pearson correlation between the Ouija pseudotimes and

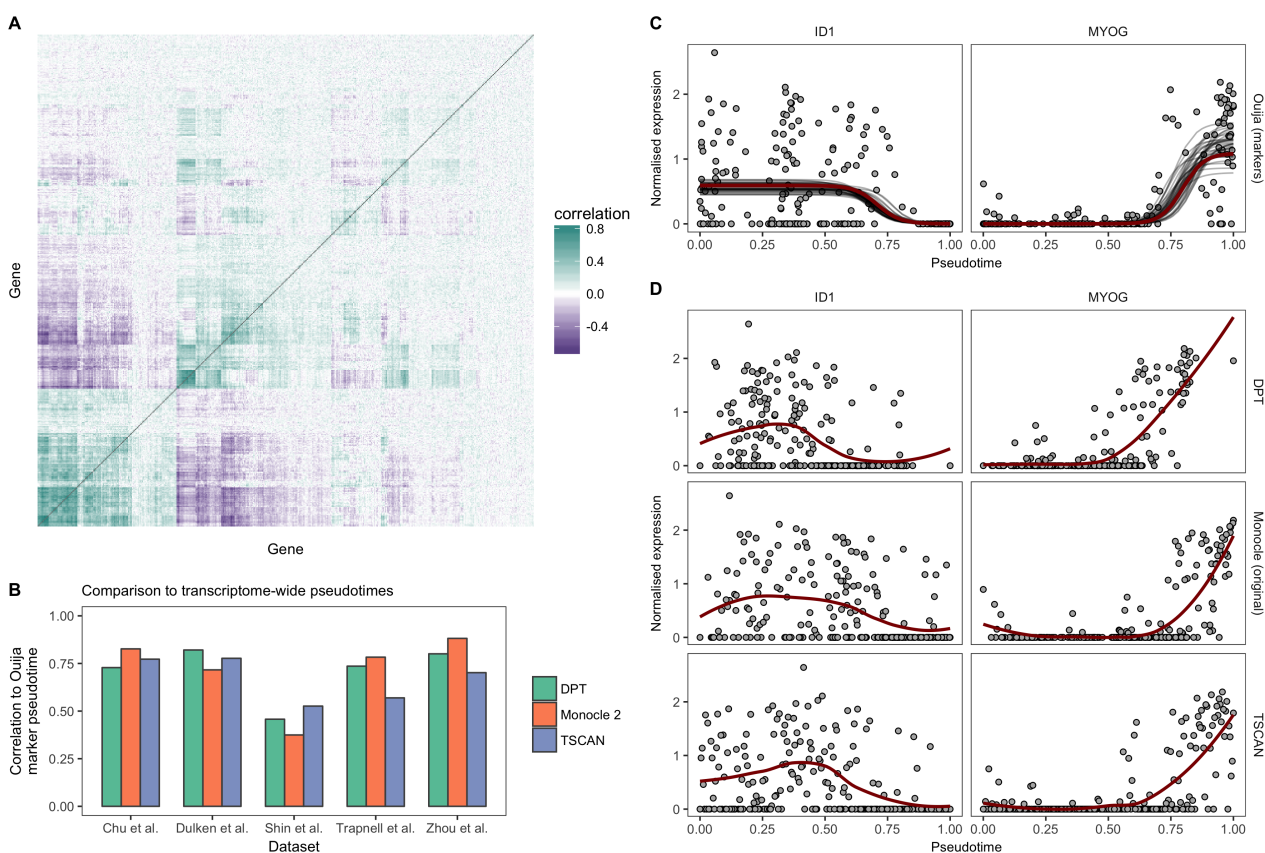


Figure 2: Transcriptome-wide pseudotimes can be inferred from small marker gene panels. A A gene-by-gene correlation matrix for the Trapnell et al. [12] dataset reveals similarities in the transcriptional response of hundreds of genes. The redundancy of expression implies the information content of the transcriptome may be compressed through techniques such as principal components analysis (PCA) or by picking informative marker genes. **B** Comparison of pseudotimes fitted using Ouija on a small panel of marker genes to transcriptome-wide fits (using the 500 most variable genes) across five datasets using the algorithms Monocle 2, DPT, and TSCAN. The marker gene fits show high correlation to the transcriptome-wide fits with the exception of the Shin et al. [20] dataset. **C** Gene expression profiles for two marker genes *ID1* and *MYOG* from the Trapnell et al. [12] dataset. The solid red line denotes the maximum *a posteriori* (MAP) Ouija fit while the grey lines show draws from the posterior mean function. **D** Gene expression profiles for the same genes for the algorithms DPT, Monocle 2, and TSCAN show similar expression fits, demonstrating equivalent pseudotemporal trajectories have been inferred. The solid red line denotes a LOESS fit.

130 the pseudotimes reported for each dataset (Figure 2B). There was good agreement between the marker-based
 131 pseudotimes inferred using Ouija and the transcriptome-wide pseudotimes inferred using existing algorithms,
 132 with the correlation exceeding 0.75 in the majority of comparisons.

133 Noting that the correlation will not be 1 unless the algorithms are identical, we sought to compare Ouija's
 134 correlation to transcriptome-wide pseudotime to the agreement of the transcriptome-wide pseudotimes with
 135 each other. We found large variability in the agreement between existing algorithms using transcriptome-wide
 136 pseudotimes, with correlations as high as 0.93 but as low as 0.61 (Supplementary Figure 2). We found the
 137 marker-based Ouija pseudotimes have higher correlations to one of the transcriptome-wide algorithms than
 138 they have amongst each other in all but one of the datasets studied. On average, the correlation between
 139 Ouija's marker based pseudotime with the transcriptome-wide pseudotimes was around 0.1 lower than the
 140 correlation amongst the transcriptome-wide pseudotimes, though given Ouija uses around 1-2% the number
 141 of input genes we believe this is a positive result that represents transcriptome-wide pseudotimes may be
 142 inferred using interpretable, parametric models on a small number of marker genes chosen *a priori*.

143 This equivalence of transcriptome-wide and marker-based pseudotimes is further confirmed by examining
 144 the qualitative fit of the marker genes across the different algorithms. For example, Figure 2C shows the
 145 posterior fit of the marker-based pseudotime for two marker genes from [12], correctly inferring the switch-like
 146 downregulation of *ID1* and the upregulation of *MYOG*. Near identical behaviour is found using transcriptome-
 147 wide pseudotimes derived from DPT, Monocle, and TSCAN (Figure 2D). We note the low correlations of the
 148 marker-based Ouija pseudotimes with the transcriptome-wide fits for the Shin et al. dataset. Upon close

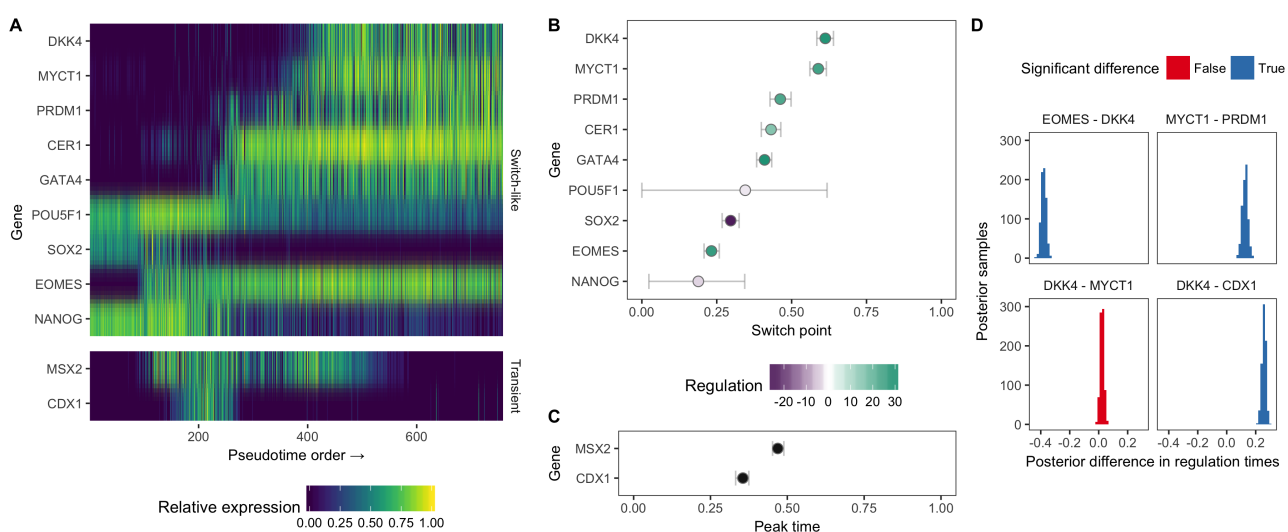


Figure 3: Parametric models lead to pseudotimes centred around gene regulation timing. **A** An expression heatmap for the 9 switch-like genes and 2 transient genes in the Chu et al. dataset, with genes ordered by the posterior mean of the switch time. **B-C** Posterior distributions over the switch times and peak times for the 11 genes, coloured by their up or down regulation along pseudotime. The horizontal error bars show the 95% highest probability density credible intervals. **D** A Bayesian hypothesis test can quantify whether the posterior difference between two regulation timings (either switch or peak time) is significantly different from 0, allowing us to determine whether a given gene is regulated before or after another along pseudotime.

149 inspection of the marker genes (Supplementary Figure 3) we found that the expression of four of the marker genes (*Aldoc*, *Apoe*, *Eomes*, *Sox11*) were highly correlated (the switch times are similar) whilst *Gfap* and 150 *Stmn1* showed little variation over pseudotime. This meant that there was effectively only a single marker gene 151 for this data set - too few for reliable marker gene-based pseudotime inference.

153 Gene regulation timing from marker gene-based pseudotime

154 Having demonstrated Ouija can accurately recapitulate transcriptome-wide pseudotimes using just small marker 155 gene panels, we next sought to show how it allows for marker-driven inference of such trajectories. Most pseu- 156 dotime inference algorithms (such as Monocle 2, DPT, TSCAN, Slicer [37]) emphasise that cells occupy a 157 low-dimensional manifold embedded in high-dimensional space and traversing this manifold corresponds to 158 following the cells over pseudotime. While such an approach is theoretically well grounded it is difficult to un- 159 derstand *why* the procedures result in a particular pseudotime trajectory, leading to the post-hoc marker gene 160 examination procedures discussed above as validation and to add interpretability.

161 To demonstrate that Ouija allows for feature-driven inference of single-cell pseudotime we applied it to a 162 single-cell time-series dataset of human embryonic stem cells differentiating into definitive endoderm cells. 163 The authors examined the expression of key marker genes over time and found 9 to exhibit approximately 164 switch-like behaviour (*POU5F1*, *NANOG*, *SOX2*, *EOMES*, *CER1*, *GATA4*, *DKK4*, *MYCT1*, and *PRDM1*) with a 165 further two exhibiting transient expression (*CDX1* and *MSX2*). We applied Ouija using noninformative priors 166 over the behaviour parameters with no information about the capture times of the cells included.

167 The resulting pseudotime fit demonstrates we can understand single-cell pseudotime in terms of the be- 168 haviour of particular genes. Figure 3A shows a heatmap of the 9 switch-like genes (top) and 2 transient genes 169 (bottom), ordered by the posterior switch time of each gene. It can be seen that the early trajectory is char- 170 acterised by the expression of *NANOG*, *SOX2*, and *POU5F1*, which then leads to a cascade of switch-like 171 activation of the remaining genes as the cells differentiate.

172 While transcriptome-wide pseudotime algorithms could provide similar heatmaps if the marker genes were 173 known in advance, the key departure of Ouija is that we can quantitatively associate each gene with a region of 174 pseudotime at which its regulation (switch time or peak time) occurs. This is illustrated in Figure 3B-C showing 175 the posterior values for the regulation timing along with the associated uncertainty. In essence, Ouija allows 176 us to order *genes* along trajectories as well as being able to order the cells, which provides insight into gene 177 regulation relationships.

178 To approach such questions of gene regulation timings in a quantitative and rigorous manner we con- 179 structed a Bayesian hypothesis test to find out whether one gene is regulated before another given the noise 180 in the data. If $t_{\text{Gene A}}^{(0)}$ and $t_{\text{Gene B}}^{(0)}$ are the regulation timings of genes A and B respectively, we calculate the

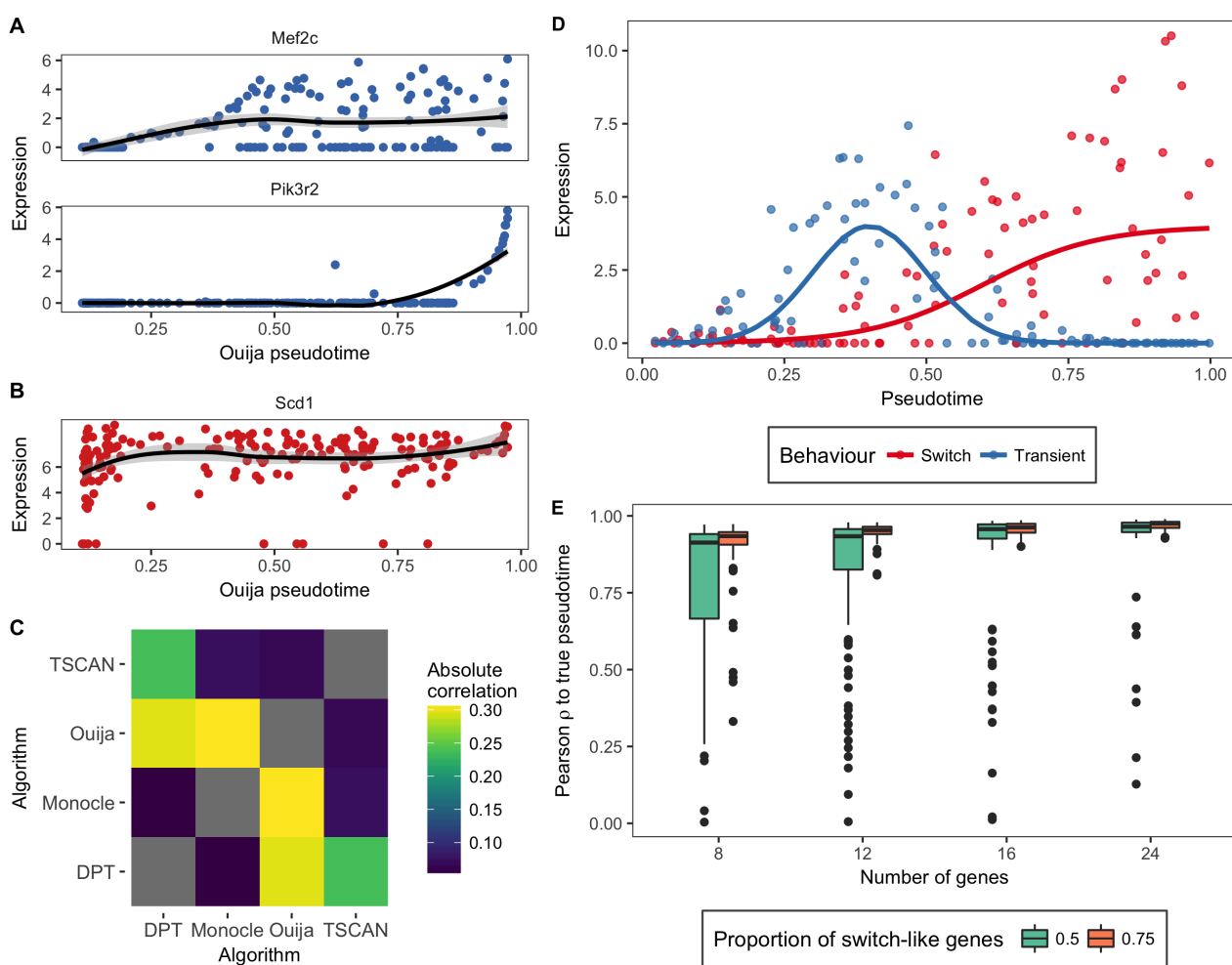


Figure 4: Ouija is robust to gene behaviour misspecification. **A** The genes *Mef2c* and *Pik3r2* show the expected behaviour in a marker-based pseudotime fitted to the Li *et al.* (2016) [32] dataset (“constant upregulation” and “transient upregulation” respectively). However, the gene *Scd1* **B** was claimed to have “tide wave” regulation (transient expression), but a LOESS fit over pseudotime (black line) shows effectively constant expression over pseudotime. **C** We found very low agreement between the different pseudotime inference algorithms for this dataset. Curiously, the largest agreement was reported between Ouija using only markers and Monocle 2 using the 500 most variable genes. **D** We simulated datasets with genes either exhibiting switch-like expression over pseudotime or transient expression, with an overdispersed, zero-inflated noise model to mimic real data. **E** Ouija was benchmarked assuming all genes were switch-like when a certain proportion were actually transient across a range of geneset sizes. Even at only 8 genes, half of which are actually transient, Ouija still recovers a median correlation of greater than 0.9 with the true pseudotime, which only increases with increasing number of genes and switch-like behaviour.

181 posterior distribution $p(t_{\text{Gene A}}^{(0)} - t_{\text{Gene B}}^{(0)} | \mathbf{Y})$, and if both the lower and upper bounds of the 95% posterior credible
 182 interval fall outside 0 we say the two genes are regulated at significantly different times. We applied this
 183 to the pseudotime fit in the Chu *et. al.* dataset, the results of which can be seen in Figure 3D for a subset of
 184 genes. The model suggests that *EOMES* is downregulated before *DKK4* and *MYCT1* is downregulated after
 185 *PRDM1*. Furthermore, it suggests the switch-like downregulation of *DKK4* occurs after the transient peak-time
 186 of *CDX1*. However, it suggests the difference in regulation timings of *DKK4* and *MYCT1* are not significantly
 187 different from zero, which could imply co-regulation.

188 Ouija is robust to gene behaviour misspecification

189 A potential disadvantage of our model is the requirement to pre-specify genes as having switch-like or transient
 190 behaviour over pseudotime, which may result in biased or erroneous pseudotimes. We noticed such an effect
 191 in the Li *et al.* (2016) [32] dataset, where the authors pre-specified how they expected several marker genes to
 192 behave over pseudotime. Upon fitting the pseudotimes using Ouija, we noted that the genes *Mef2c* and *Pik3r2*
 193 exhibited the correct upregulation over pseudotime (Figure 4A), but that *Scd1* that was supposed to exhibit

194 transient, peaking expression was effectively constant along the trajectory (Figure 4B).

195 We first sought to discover whether this was a particular failing of Ouija or a result common to all pseu-
196 dotime algorithms. To do so, we fitted transcriptome-wide pseudotimes using TSCAN, Monocle 2 and DPT,
197 and compared both the correlation among the different algorithms and the behaviour of the specified marker
198 genes. We found remarkably low correlations between the different pseudotime algorithms (Figure 4C), with
199 the highest correlations reported between Ouija using markers only and Monocle 2 using the full transcrip-
200 tome. Furthermore, none of the pseudotime fits displays consistent nor expected behaviour for the set of
201 marker genes (Supplementary Figure 4). For example, the gene *Foxa2* is seemingly downregulated under DPT,
202 upregulated under Monocle 2 and Ouija, and exhibits transient expression under TSCAN.

203 Next, we performed extensive simulations to discover the extent to which Ouija is in general robust to gene
204 behaviour misspecification. We simulated datasets where either 75% or 50% of the genes were switch-like
205 (Figure 4D) for 8, 12, 16 & 24 genes with 100 replications for each situation, and re-inferred the pseudotimes
206 using Ouija assuming all genes were switch-like. The results can be seen in Figure 4D. Even with 4 switch-like
207 and 4 transient genes Ouija still achieves a median correlation greater than 0.9 with the true pseudotimes, a
208 result that only increases with more switch-like genes. We believe this shows that Ouija is highly robust to
209 misspecification of prior knowledge of gene behaviour.

210 It is further possible to identify errors in the prior belief of gene behaviour without having to explicitly fit a
211 pseudotemporal trajectory. If a dataset contains a number of switch-like and transient genes, the switch-like
212 genes will have high absolute correlation with themselves but low absolute correlation with the transient genes,
213 which will in turn have high absolute correlation with themselves. This effect is exemplified in the Chu *et al.*
214 dataset that contains 9 switch-like and 2 transient genes. A hierarchical clustering of the absolute correlations
215 across the genes reveals the transient genes clustering separately from the switch-like genes (Supplementary
216 Figure 5). Therefore, an investigator could corroborate their prior expectations through similar investigations.

217 Identifying discrete cell types along continuous developmental trajectories

218 We further investigated the single cell expression data from a study tracking the differentiation of embryonic
219 precursor cells into haematopoietic stem cells (HSCs) [33]. The cells begin as haemogenic endothelial cells
220 (ECs) before successively transforming into pre-HSC and finally HSC cells. The authors identified six marker
221 genes that would be down-regulated along the differentiation trajectory, with early down-regulation of *Nrp2*
222 and *Nr2f2* as the cells transform from ECs into pre-HSCs, and late down-regulation of *Nrp1*, *Hey1*, *Efnb2* and
223 *Ephb4* as the cells emerge from pre-HSCs to become HSCs. The study investigated a number of distinct
224 cell types at different stages of differentiation: EC cells, T1 cells (*CDK45*⁻ pre-HSCs), T2 cells (*CDK45*⁺
225 pre-HSCs) and HSC cells at the E12 and E14 developmental stages.

226 We therefore sought to identify the existence of these discrete cell types along the continuous developmen-
227 tal trajectory. As Ouija uses a probabilistic model and inference we were able to obtain a posterior ordering
228 “consistency” matrix (Figure 5A) where an entry in row *i* column *j* denotes the empirical probability that cell
229 *i* is ordered before cell *j*. Performing PCA on this matrix gives a rank-one representation of cell-cell continu-
230 ity, which is then clustered using a Gaussian mixture model to find discrete cell states along the continuous
231 trajectory (where the number of states is chosen such that the Bayesian information criterion is maximised).

232 Applying this methodology to the Zhou *et. al.* dataset uncovered three metastable groups of cells cor-
233 responding to endothelial, pre-HSCs and HSCs respectively (Figure. 5B). Misclassifications within cell types
234 (T1/T2 and E12/E14 cells) could be explained by examining a principal components analysis of the global
235 expression profiles (Supplementary Figure 6) which suggests that these cell types are not completely distinct
236 in terms of expression. When examining the inferred pseudotime progression of each marker gene (Figure
237 5C), these three metastable states corresponded to the activation of all genes at the beginning of pseudotime
238 time, the complete inactivation of all the marker genes at the end of the pseudotime and a intervening tran-
239 sitory period as each marker gene turns off. Each metastable state clearly associates with a particular cell
240 type with *Nrp2* and *Nr2f2* exhibiting early down-regulation and *Nrp1*, *Hey1*, *Efnb2* and *Ephb4* all exhibiting late
241 down-regulation. Using this HSC formation system as a proof-of-principle it is evident that, if a small number
242 of switch-like marker genes are known, it is possible to recover signatures of temporal progression using Ouija
243 and that these trajectories are compatible with real biology.

244 To show the widespread applicability of this method we applied it to two further publically available datasets.
245 Dulken *et. al.* [34] examined the trajectory of quiescent neural stem cells (qNSCs) as they differentiate into
246 activated neural stem cells (aNSCs) and neural progenitor cells (NPCs). Applying Ouija’s clustering-along-
247 pseudotime revealed seven distinct clusters (Supplementary Figure 7; Supplementary Table 1) with clusters
248 1-2 corresponding to early and late qNSCs, cluster 3 defining the qNSC to aNSC transition, clusters 4-6 cor-
249 responding to early to late aNSCs and cluster 7 defining the aNSC to NPC transition. We similarly applied this
250 method to the Chu *et al.* dataset of time-series scRNA-seq that identified 8 distinct clusters along pseudotime
251 (Supplementary Figure 8; Supplementary Table 2). Clusters 1-4 track the cells as the progress through the

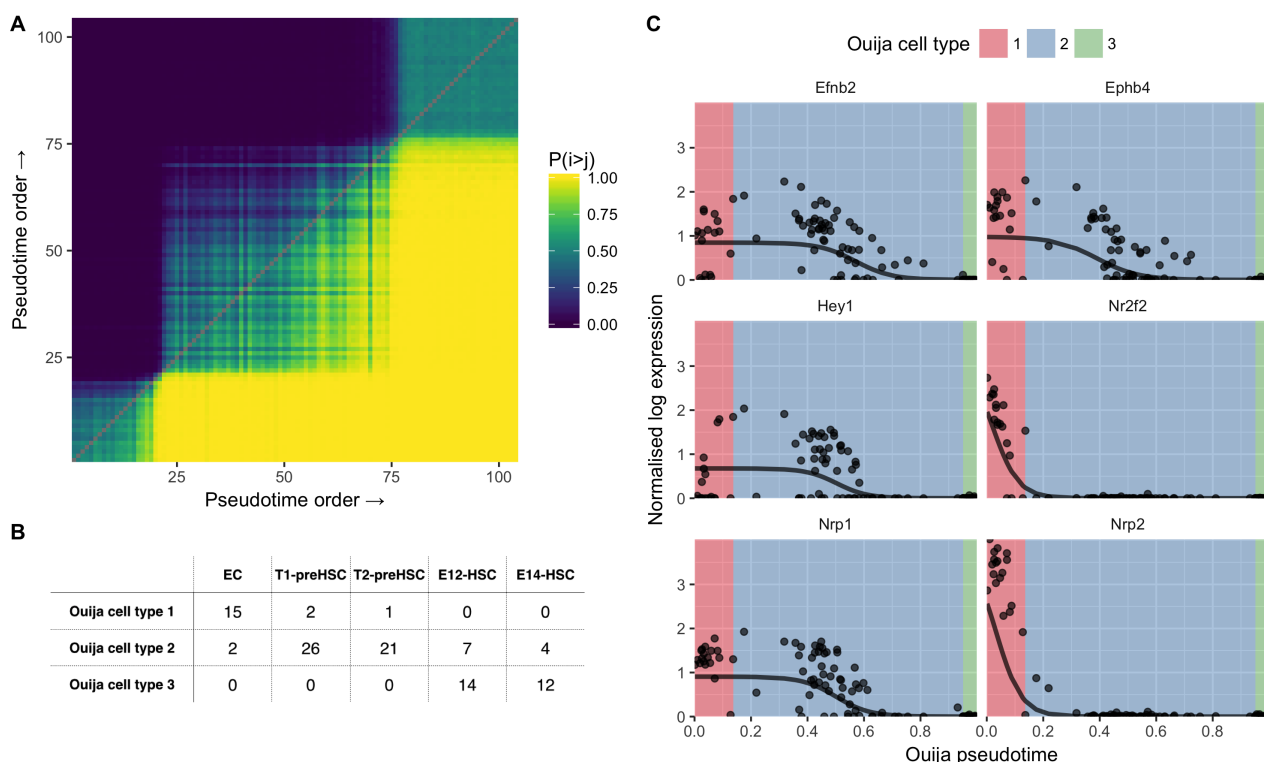


Figure 5: Pseudotime ordering and cell type identification of haematopoietic stem cell differentiation

A Consistency matrix of pseudotime ordering. Entry in the i^{th} row and j^{th} column is the proportion of times cell i was ordered before cell j in the MCMC posterior traces. Gaussian mixture modelling on the first principal component of the matrix identified three clusters that are evident in the heatmap. **B** Confusion matrix for cell types identified in original study (columns) and Ouija inferred (rows). Ouija inferred cluster 1 largely corresponds to EC cells, cluster 2 corresponds to pre-HSC cells while cluster 3 corresponds to HSC cells. **C** HSC gene expression as a function of pseudotime ordering for six marker genes. Background colour denotes the maximum likelihood estimate for the Ouija inferred cell type in that region of pseudotime.

252 4 stages from 0 hours to 36 hours, while clusters 5-8 track the 3 stages from 36 hours to 96h hours but with
 253 much more heterogeneity within each cluster, which is expected due to the longer time-scales considered.

254 Incorporating prior information can improve pseudotime inference

255 A particular advantage of using Bayesian models with interpretable parameters is that we may express any prior
 256 knowledge about the gene behaviour as informative priors. For example, for each gene we model as switch-
 257 like there is the switch strength parameter k that models how quickly a gene is upregulated if k is positive or
 258 how quickly it is downregulated if it is negative. A researcher may have a firm prior belief that a gene will be
 259 up or downregulated along the trajectory and thus can place a prior $p(k)$ on the particular parameters. Using
 260 Bayes' rule, the posterior distribution of both the pseudotimes and gene-specific parameters is then calculated
 261 by combining this informative prior with the data likelihood. The crucial observation here is that the posterior
 262 distribution of the pseudotimes is affected by priors on the gene behaviour parameters, meaning incorporating
 263 prior information about gene behaviours may improve pseudotime inference. Such informative priors may be
 264 placed on any of the parameters that govern interpretable gene behaviour. For example, if a researcher expects
 265 a particular transient gene to peak early in the trajectory then they may encode this using a prior distribution
 266 on the peak time.

267 We sought to test the extent to which incorporating knowledge of gene behaviours through informative
 268 Bayesian priors aids pseudotime inference. To do so we performed extensive simulations of single-cell pseu-
 269 dotime under monotonic changes in expression and reinferred using Ouija with both noninformative and infor-
 270 mative priors, as well as DPT and TSCAN. In order to emulate the fact that the data will not truly come from
 271 a sigmoidal link function, we simulated data from various link functions used in logistic regression including
 272 probit and complementary log-log (Figure 6) along with a "threshold" model where the expression is on or off
 273 with a particular probability that changes along the trajectory (see supplementary text for full details).

274 The results can be seen in Figure 6, with similar characteristics across the four mean functions considered.
 275 In all cases Ouija performs substantially better than DPT and TSCAN, but we note that this is likely due to the

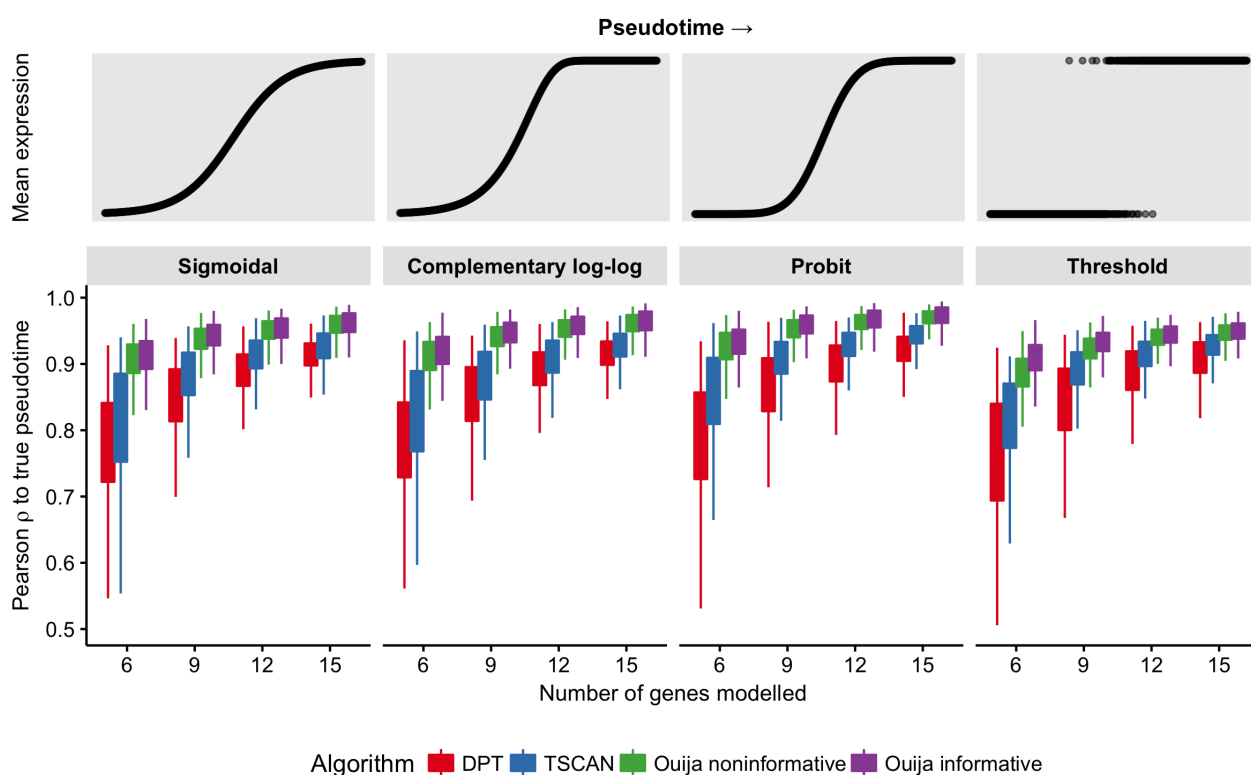


Figure 6: Incorporating prior information can improve pseudotime inference. We sought to identify the benefits of incorporating prior information about the behaviour of genes to the accuracy of pseudotime inference. We simulated data according to four different mean functions (sigmoidal, complementary log-log, probit, and threshold) under identical noise model and reinferrred using DPT, TSCAN, Ouija with noninformative priors, and Ouija with informative priors. The results show a marginal though significant gain in inference when incorporating prior knowledge.

276 data generating model more closely matching the likelihood model of Ouija though could also be explained
 277 by the fact that DPT and TSCAN are not designed for small panels of genes. In each case the gain from
 278 incorporating prior information is statistically significant (Supplementary Table 3), but we note that the effect
 279 sizes are in practice quite small. Since to infer a consistent pseudotime, sufficient correlations must exist in the
 280 data, prior knowledge may only make a relatively minor contribution. However, researchers dealing with data
 281 with low biological signal to noise ratio may find it advantageous to incorporate such constraints to improve the
 282 quality of their inferences.

283 Scalable pseudotime inference using TensorFlow

284 Finally, we wanted to consider a study composed of a large panel of putative marker genes to determine if Ouija
 285 could automatically identify genes satisfying its behavioural constraints. We identified a single-cell RNA-seq
 286 study [38] that examined variation between individual hematopoietic stem and progenitor cells from two mouse
 287 strains (C57BL/6 and DBA/2) as they age. Principal component analysis for each cell type and age showed
 288 a striking association of the top principal components with cell cycle-related genes (Figure 7A), indicating that
 289 transcriptional heterogeneity was dominated by cell cycle status. They scored each cell for its likely cell cycle
 290 phase using signatures based on functional annotations [39] and profiles from synchronized HeLa cells [40]
 291 for the G1/S, S, G2, and G2/M phases.

292 We investigated if Ouija could be used to identify cell cycle phase, treating the inferential problem as a con-
 293 tinuous pseudotime process and assuming all genes as candidate switch genes. We applied Ouija to 1,008
 294 C57BL/6 HSCs using 374 GO cell cycle genes that satisfied gene selection criteria used in the original study.
 295 This large number of genes and cells makes inference using Hamiltonian Monte Carlo (HMC) slow so we imple-
 296 mented a second version of Ouija (termed *Ouijafow*) using the probabilistic programming language Edward
 297 [41] based on TensorFlow [42]. This performs fast approximate Bayesian inference using reparametrization
 298 gradient variational inference.

299 The estimated pseudotime progression given by Ouija recapitulates the trajectory observed in principal
 300 component space (Figure 7A). The estimated pseudotime distribution correlates well with the cell cycle phase

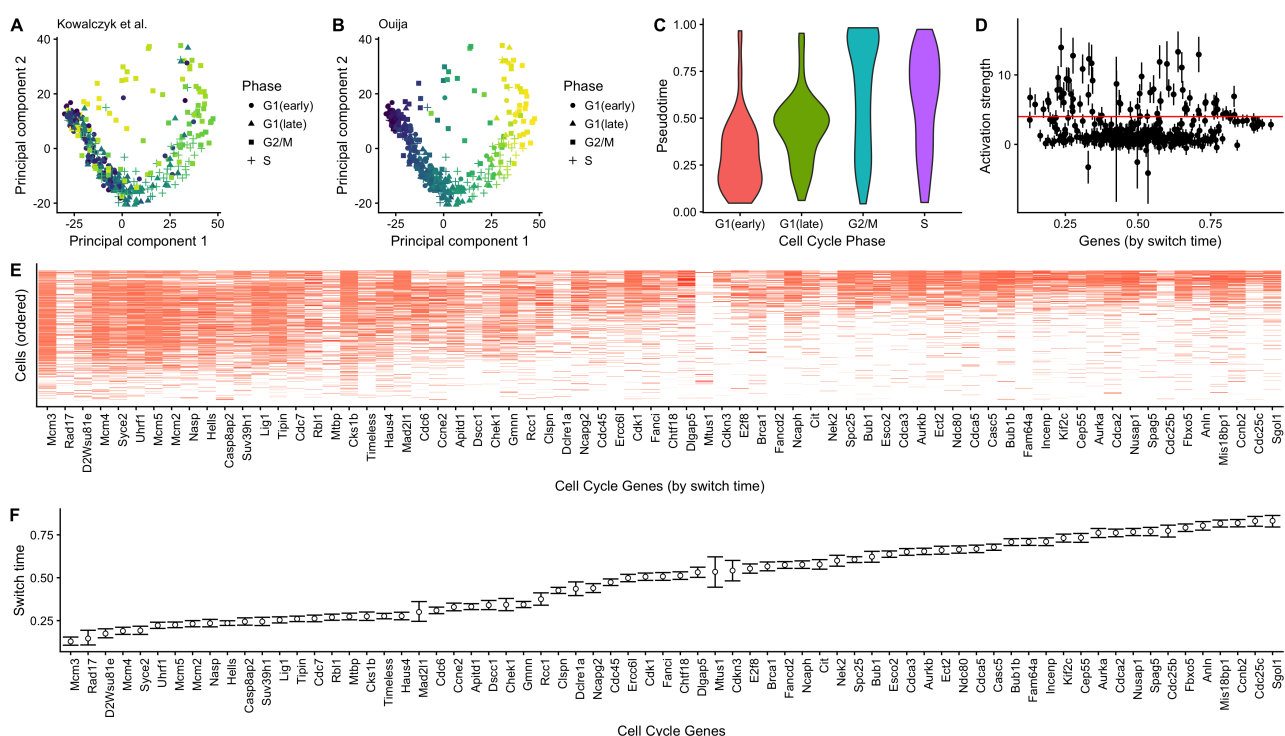


Figure 7: Cell cycle phase prediction. Principal component representation of hematopoietic stem cells coloured according to (A) the original cell cycle progression score [38] and (B) Ouija - cell cycle classes indicated are based on original study classifications. (C) Distribution of Ouija inferred pseudotime versus the original cell cycle classifications. (D) Estimated activation strengths for the 374 cell cycle gene panels. (E) Gene expression profile for 88 switch-like genes with cells ordered by pseudotime and (F) genes ordered by activation time.

301 categorisation given in the original study (Figure 7C). Furthermore, we identified 88 genes with large activation
 302 strengths indicating strong switching-on behaviour (Figure 7D). Ordering the genes by activation time
 303 demonstrates a cascade of expression activation across these 88 genes over cell cycle progression with the
 304 quiescent (G_0) indicated by complete inactivation of all 88 genes (Figure 7E,F). The explicit parametric model
 305 assumed by Ouija makes this gene selection and ordering process simple and *quantitative* compared to a
 306 non-parametric approach that would require some retrospective analysis or visual inspection.

307 Conclusions

308 We have developed a novel approach for pseudotime estimation based on modelling switch-like and transient
 309 expression behaviour for a small panel of marker genes chosen *a priori*. Our strategy provides an orthogonal
 310 and complimentary approach to unsupervised whole-transcriptome methods that do not explicitly model any
 311 gene-specific behaviours and do not readily permit the inclusion of prior knowledge.

312 We demonstrate that the selection of a few marker genes allows comparable pseudotime estimates to whole
 313 transcriptome methods on real single cell data sets. Furthermore, using a parametric gene behaviour model
 314 and full Bayesian inference we are able to recover posterior uncertainty information about key parameters,
 315 such as the gene activation time, allowing us to explicitly determine a potential ordering of gene (de)activation
 316 and peaking events over (pseudo)time. The posterior ordering uncertainty can also be used to identify ho-
 317 mogeneous metastable phases of transcriptional activity that might correspond to transient, but discrete, cell
 318 states.

319 Furthermore, whilst we do not explicitly address branching processes in this work, our framework provides
 320 a natural and simple extension to allow for multiple lineages and cell fates using a sparse mixture of factor
 321 analyzers in which each lineage is denoted by a separate mixture component and the factors loadings are
 322 shrunk to common values to denote shared branches. This has been explored in work elsewhere [43].

323 In summary, Ouija provides a novel contribution to the increasing plethora of pseudotime estimation meth-
 324 ods available for single cell gene expression data.

325 Methods

326 Overview

We give a high-level overview of our pseudotime inference framework here and provide more technical details in the following sub-sections. The aim of pseudotime ordering is to associate a p -dimensional expression measurement (the data) to a latent unobserved pseudotime. Mathematically we can express this as the following:

$$\underbrace{y_n}_{\text{Expression}} = \underbrace{f}_{\text{Mapping}} \left(\underbrace{t_n}_{\text{Pseudotime}} \right) + \underbrace{\epsilon_n}_{\text{Noise}} \quad (1)$$

327 where the function f maps the one-dimensional pseudotime t_n for cell n to the p -dimensional observation space
 328 in which the data lies. The challenge lies in the fact that *both* the mapping function f and the pseudotimes are
 329 *unknown*. Our objective here is to use parametric forms for the mapping function f that will enable relatively
 330 fast computations whilst characterising certain gene expression temporal behaviours. The specification of a
 331 statistical pseudotime algorithm therefore comes down to the choice of the mean function f and the noise
 332 model on ϵ that we detail below.

333 The approach we adopt is therefore a form of latent variable model implemented as *non-linear parametric*
 334 *factor analysis* where the factors correspond to the pseudo-times and the factor loadings correspond to the
 335 interpretable parameters of the sigmoidal or transient mean functions that provide the non-linearity. In addition,
 336 we model dropouts and a strict empirically motivated mean-variance relationship which is required to provide
 337 constraints on the latent variable model since nothing on the right hand side of equation 1 is actually measured
 338 or observed.

339 Statistical model

340 Input data normalisation

341 We index N cells by $n \in 1, \dots, N$ and G genes by $g \in 1, \dots, G$. Let $y_{ng} = [\mathbf{Y}]_{ng}$ denote the log-transformed
 342 non-negative observed cell-by-gene expression matrix. In order to make the strength parameters comparable
 343 between genes we normalise the gene expression so the approximate half-peak expression is 1 through the
 344 transformation

$$\mathbf{y}_g \rightarrow \mathbf{y}_g / s_g. \quad (2)$$

345 where s_g is a gene-specific size factor defined by

$$s_g = \frac{1}{|\mathcal{Y}_g^*|} \sum_{y_{cg}^* \in \mathcal{Y}_g^*} y_{cg}^* \quad (3)$$

346 and $\mathcal{Y}_g^* = \{y_{cg} : y_{cg} > 0\}$.

347 Noise model

Our statistical model can be specified as a Bayesian hierarchical model where the likelihood is given by a bimodal distribution formed from a mixture of zero-component (dropout) and an non-zero expressing cell population. If $\mu(t_n, \Theta_g)$ is the mean for cell n and gene g (evaluated at pseudotime t_n with gene-specific parameters Θ_g) then

$$y_{ng} \sim \begin{cases} \theta_{ng} + (1 - \theta_{ng})\text{Student}(\mu(t_n, \Theta_g), \sigma_{ng}^2) & \text{if } y_{ng} = 0 \\ (1 - \theta_{ng})\text{Student}(\mu(t_n, \Theta_g), \sigma_{ng}^2) & \text{if } y_{ng} > 0 \end{cases}, \quad (4)$$

$$\theta_{ng} \sim \text{Bernoulli}(\text{logit}^{-1}(\beta_0 + \beta_1 \mu(t_n, \Theta_g))), \quad (5)$$

$$\beta \sim \text{Normal}(0, 0.1). \quad (6)$$

348 The relationship between dropout rate and expression level is expressed as a logistic regression model
 349 [44]. Furthermore, we impose a mean-variance relationship of the form:

$$\sigma_{ng}^2 = (1 + \phi)\mu(t_n, \Theta_g) + \epsilon \quad (7)$$

350 where ϕ is the dispersion parameter with prior $\phi \sim \text{Gamma}(\alpha_\phi, \beta_\phi)$, which is motivated by empirical obser-
 351 vations of marker gene behaviour (see supplementary text).

352 **Mean functions**

353 We then need to specify the form of the mean functions $\mu(t_n, \Theta_g)$, for which we consider both sigmoidal and
354 transient genes.

355 For the sigmoidal case we have

$$\mu(t_n, \Theta_g) = f_{\text{Sigmoidal}}(t_n; k_g, t_g^{(0)}, \mu_g^{(0)}) = \frac{2\mu_g^{(0)}}{1 + \exp\left(-k_g(t_c - t_g^{(0)})\right)}, \quad (8)$$

where k_g and $t_g^{(0)}$ denote the activation strength and activation time parameters for each gene and $\mu_g^{(0)}$ the average peak expression with default priors

$$\mu_g^{(0)} \sim \text{Gamma}(\delta/2, 1/2), \quad (9)$$

$$k_g \sim \text{Normal}(\mu_g^{(k)}, 1/\tau_g^{(k)}), \quad (10)$$

$$t_g^{(0)} \sim \text{TruncNorm}_{[0,1]}(\mu_g^{(t)}, 1/\tau_g^{(t)}), \quad (11)$$

356 If available, user-supplied prior beliefs can be encoded in these priors by specifying the parameters $\mu_g^{(k)}, \tau_g^{(k)}, \mu_g^{(t)}, \tau_g^{(t)}$.
357 Otherwise, inference can be performed using uninformative hyperpriors on these parameters. Specifying $\mu_g^{(k)}$
358 encodes a prior belief in the strength and direction of the activation of gene g along the trajectory with $\tau_g^{(k)}$
359 (inversely-) representing the strength of this belief. Similarly, specifying $\mu_g^{(t)}$ encodes a prior belief of where in
360 the trajectory gene g exhibits behaviour (either turning on or off) with $\tau_g^{(t)}$ encoding the strength of this belief.

361 For the transient case we have

$$\mu(t_n, \Theta_g) = f_{\text{Transient}}(t_n; p_g, b_g, \mu_g^{(0)}) = 2\mu_g^{(0)} \exp(-\lambda b_g(t_n - p_g)^2), \quad (12)$$

where we take λ to be a constant $\lambda = 10$ and with a prior structure

$$\mu_g^{(0)} \sim \text{Gamma}(\delta/2, 1/2), \quad (13)$$

$$p_g \sim \text{TruncNorm}_{[0,1]}(\mu_g^{(p)}, 1/\tau_g^{(p)}), \quad (14)$$

$$b_g \sim \text{TruncNorm}_{[0,\infty)}(\mu_g^{(p)}, 1/\tau_g^{(p)}), \quad (15)$$

362 where informative priors may be placed on p and b as before.

363 Note that if the mapping functions f are restricted to a linear form then the model reduces to Factor Anal-
364 ysis. In other words, performing factor analysis on single-cell RNA-seq data is entirely equivalent to finding
365 a trajectory where gene expression is linear over time with no prior expectations on how the genes behave.
366 If we model a common precision across all genes so $\tau_g = \tau$ then the model reduces further to probabilistic
367 principal components analysis [45], providing an explicit interpretation for the results of principal component
368 analysis on single-cell data.

369 **Inference**

370 We performed posterior inference using Markov Chain Monte Carlo (MCMC) stochastic simulation algorithms,
371 specifically the No U-Turn Hamiltonian Monte Carlo approach [46] implemented in the STAN probabilistic pro-
372 gramming language [47] which we use to implement our model. The parameter $\epsilon = 0.01$ is used to avoid
373 numerical issues in MCMC computation. For larger marker gene panels, such as in the cell cycle analysis
374 section, we used the reparametrization gradient variational inference methods implemented in Edward [41] to
375 perform approximate Bayesian inference.

376 **Competing interests**

377 The authors declare that they have no competing interests.

378 **Author's contributions**

379 K.R.C. and C.Y. conceived the study. K.R.C. developed software and performed computer simulations. K.R.C.
380 and C.Y. wrote the manuscript.

381 Acknowledgements

382 K.R.C. is supported by a UK Medical Research Council funded doctoral studentship. C.Y. is supported by a UK
383 Medical Research Council New Investigator Research Grant (Ref. No. MR/L001411/1), the Wellcome Trust
384 Core Award Grant Number 090532/Z/09/Z, the John Fell Oxford University Press (OUP) Research Fund and
385 the Li Ka Shing Foundation via a Oxford-Stanford Big Data in Human Health Seed Grant.

386 References

- 387 [1] Tomer Kalisky and Stephen R Quake. "Single-cell genomics". In: *Nature methods* 8.4 (2011), pp. 311–
388 314.
- 389 [2] Ehud Shapiro, Tamir Biezuner, and Sten Linnarsson. "Single-cell sequencing-based technologies will
390 revolutionize whole-organism science." In: *Nature reviews. Genetics* 14.9 (Sept. 2013), pp. 618–30. ISSN:
391 1471-0064. DOI: 10.1038/nrg3542. URL: <http://www.ncbi.nlm.nih.gov/pubmed/23897237>.
- 392 [3] Iain C Macaulay and Thierry Voet. "Single cell genomics: advances and future perspectives." In: *PLoS
393 genetics* 10.1 (Jan. 2014), e1004126. ISSN: 1553-7404. DOI: 10.1371/journal.pgen.1004126. URL:
394 <http://www.ncbi.nlm.nih.gov/articlerender.fcgi?artid=3907301&tool=pmcentrez&rendertype=abstract>.
- 395 [4] Quin F Wills and Adam J Mead. "Application of Single Cell Genomics in Cancer: Promise and Chal-
396 lenges". In: *Human molecular genetics* (2015), p. ddv235.
- 397 [5] Sten Linnarsson and Sarah A Teichmann. "Single-cell genomics: coming of age". In: *Genome biology*
398 17.1 (2016), p. 1.
- 399 [6] Serena Liu and Cole Trapnell. "Single-cell transcriptome sequencing: recent advances and remaining
400 challenges". In: *F1000Research* 5 (2016).
- 401 [7] Oliver Stegle, Sarah a. Teichmann, and John C. Marioni. "Computational and analytical challenges in
402 single-cell transcriptomics". In: *Nature Reviews Genetics* 16.3 (Jan. 2015), pp. 133–145. ISSN: 1471-
403 0056. DOI: 10.1038/nrg3833. URL: <http://www.nature.com/doifinder/10.1038/nrg3833>.
- 404 [8] Cole Trapnell. "Defining cell types and states with single-cell genomics". In: *Genome Res* 25.10 (2015),
405 pp. 1491–8. DOI: 10.1101/gr.190595.115.
- 406 [9] Peng Qiu et al. "Extracting a cellular hierarchy from high-dimensional cytometry data with SPADE". In:
407 *Nature biotechnology* 29.10 (2011), pp. 886–891.
- 408 [10] Sean C Bendall et al. "Single-cell trajectory detection uncovers progression and regulatory coordina-
409 tion in human B cell development." In: *Cell* 157.3 (Apr. 2014), pp. 714–25. ISSN: 1097-4172. DOI:
410 10.1016/j.cell.2014.04.005. URL: <http://www.sciencedirect.com/science/article/pii/S0092867414004711>.
- 411 [11] Eugenio Marco et al. "Bifurcation analysis of single-cell gene expression data reveals epigenetic land-
412 scape." In: *Proceedings of the National Academy of Sciences of the United States of America* 111.52
413 (Dec. 2014), E5643–50. ISSN: 1091-6490. DOI: 10.1073/pnas.1408993111. URL: <http://www.ncbi.nlm.nih.gov/articlerender.fcgi?artid=4284553&tool=pmcentrez&rendertype=abstract>.
- 414 [12] Cole Trapnell et al. "The dynamics and regulators of cell fate decisions are revealed by pseudotemporal
415 ordering of single cells." In: *Nature biotechnology* 32.4 (Apr. 2014), pp. 381–6. ISSN: 1546-1696. DOI:
416 10.1038/nbt.2859. URL: <http://www.ncbi.nlm.nih.gov/pubmed/24658644>.
- 417 [13] Victoria Moignard et al. "Decoding the regulatory network of early blood development from single-cell
418 gene expression measurements". In: *Nature Biotechnology* 33.3 (Feb. 2015). ISSN: 1087-0156. DOI:
419 10.1038/nbt.3154. URL: <http://www.nature.com/doifinder/10.1038/nbt.3154>.
- 420 [14] John E Reid and Lorenz Wernisch. "Pseudotime estimation: deconfounding single cell time series". In:
421 *bioRxiv* (2015), p. 019588.
- 422 [15] N. K. Hanchate et al. "Single-cell transcriptomics reveals receptor transformations during olfactory neu-
423 rogenesis". In: *Science* (Nov. 2015), science.aad2456–. ISSN: 0036-8075. DOI: 10.1126/science.aad2456.
424 URL: <http://www.sciencemag.org/content/early/2015/11/04/science.aad2456.full>.
- 425 [16] Jaehoon Shin et al. "Single-Cell RNA-Seq with Waterfall Reveals Molecular Cascades underlying Adult
426 Neurogenesis". English. In: *Cell Stem Cell* 17.3 (Aug. 2015), pp. 360–372. ISSN: 19345909. DOI: 10.
427 1016/j.stem.2015.07.013. URL: <http://www.cell.com/article/S1934590915003124/fulltext>.
- 428 [17] Laleh Haghverdi, Maren Buettnner, F Alexander Wolf, Florian Buettnner, and Fabian J Theis. "Diffusion
429 pseudotime robustly reconstructs lineage branching". In: *Nature Methods* (2016).

433 [18] Zhicheng Ji and Hongkai Ji. "TSCAN: Pseudo-time reconstruction and evaluation in single-cell RNA-seq
434 analysis". In: *Nucleic acids research* (2016), gkw430.

435 [19] Manu Setty et al. "Wishbone identifies bifurcating developmental trajectories from single-cell data". In:
436 *Nature biotechnology* 34.6 (2016), pp. 637–645.

437 [20] Jaehoon Shin et al. "Single-cell RNA-seq with waterfall reveals molecular cascades underlying adult
438 neurogenesis". In: *Cell stem cell* 17.3 (2015), pp. 360–372.

439 [21] Allison N Tegge, Charles W Caldwell, and Dong Xu. "Pathway correlation profile of gene-gene co-
440 expression for identifying pathway perturbation". In: *PLoS one* 7.12 (2012), e52127.

441 [22] Rosemary Braun, Leslie Cope, and Giovanni Parmigiani. "Identifying differential correlation in gene/pathway
442 combinations". In: *BMC bioinformatics* 9.1 (2008), p. 488.

443 [23] Peter Langfelder and Steve Horvath. "WGCNA: an R package for weighted correlation network analysis".
444 In: *BMC bioinformatics* 9.1 (2008), p. 559.

445 [24] Graham Heimberg, Rajat Bhatnagar, Hana El-Samad, and Matt Thomson. "Low dimensionality in gene
446 expression data enables the accurate extraction of transcriptional programs from shallow sequencing".
447 In: *Cell systems* 2.4 (2016), pp. 239–250.

448 [25] Brian Cleary, Le Cong, Eric Lander, and Aviv Regev. "Composite measurements and molecular com-
449 pressed sensing for highly efficient transcriptomics". In: *bioRxiv* (2017), p. 091926.

450 [26] Shannon McCurdy, Vasilis Ntranos, and Lior Pachter. "Column subset selection for single-cell RNA-Seq
451 clustering". In: *bioRxiv* (2017), p. 159079.

452 [27] L. Haghverdi, F. Buettner, and F. J. Theis. "Diffusion maps for high-dimensional single-cell analysis of dif-
453 ferentiation data". In: *Bioinformatics* May (2015), pp. 1–10. ISSN: 1367-4803. DOI: 10.1093/bioinformatics/
454 btv325. URL: <http://www.ncbi.nlm.nih.gov/pubmed/26002886>.

455 [28] Emma Pierson and Christopher Yau. "ZIFA: Dimensionality reduction for zero-inflated single-cell gene
456 expression analysis". In: *Genome biology* 16.1 (2015), pp. 1–10.

457 [29] Kieran R Campbell and Christopher Yau. "Probabilistic modeling of bifurcations in single-cell gene ex-
458 pression data using a Bayesian mixture of factor analyzers". en. In: *Wellcome Open Res* 2 (2017), p. 19.

459 [30] Kieran R Campbell and Christopher Yau. "Order Under Uncertainty: Robust Differential Expression Anal-
460 ysis Using Probabilistic Models for Pseudotime Inference". en. In: *PLoS Comput. Biol.* 12.11 (Nov. 2016),
461 e1005212.

462 [31] Kieran R Campbell and Christopher Yau. "switchde: inference of switch-like differential expression along
463 single-cell trajectories". en. In: *Bioinformatics* (2016).

464 [32] Junxiang Li et al. "Systematic reconstruction of molecular cascades regulating GP development using
465 single-cell RNA-seq". In: *Cell reports* 15.7 (2016), pp. 1467–1480.

466 [33] Fan Zhou et al. "Tracing haematopoietic stem cell formation at single-cell resolution". In: *Nature* 533.7604
467 (2016), pp. 487–492.

468 [34] Ben W Dulken, Dena S Leeman, Stéphane C Boutet, Katja Hebestreit, and Anne Brunet. "Single-cell
469 transcriptomic analysis defines heterogeneity and transcriptional dynamics in the adult neural stem cell
470 lineage". In: *Cell reports* 18.3 (2017), pp. 777–790.

471 [35] Li-Fang Chu et al. "Single-cell RNA-seq reveals novel regulators of human embryonic stem cell differen-
472 tiation to definitive endoderm". In: *Genome biology* 17.1 (2016), p. 173.

473 [36] Davis J McCarthy, Kieran R Campbell, Aaron T L Lun, and Quin F Wills. "Scater: pre-processing, quality
474 control, normalization and visualization of single-cell RNA-seq data in R". en. In: *Bioinformatics* (2017).

475 [37] Joshua D Welch, Alexander J Hartemink, and Jan F Prins. "SLICER: inferring branched, nonlinear cellu-
476 lar trajectories from single cell RNA-seq data". In: *Genome biology* 17.1 (2016), p. 106.

477 [38] Monika S Kowalczyk et al. "Single-cell RNA-seq reveals changes in cell cycle and differentiation pro-
478 grams upon aging of hematopoietic stem cells". In: *Genome research* 25.12 (2015), pp. 1860–1872.

479 [39] Reference Genome Group of the Gene Ontology Consortium et al. "The Gene Ontology's Reference
480 Genome Project: a unified framework for functional annotation across species". In: *PLoS Comput Biol*
481 5.7 (2009), e1000431.

482 [40] Michael L Whitfield et al. "Identification of genes periodically expressed in the human cell cycle and their
483 expression in tumors". In: *Molecular biology of the cell* 13.6 (2002), pp. 1977–2000.

484 [41] Dustin Tran, Alp Kucukelbir, Adji B Dieng, Maja Rudolph, Dawen Liang, and David M Blei. "Edward: A
485 library for probabilistic modeling, inference, and criticism". In: (Oct. 2016). arXiv: 1610.09787 [stat.CO].

486 [42] Martín Abadi et al. “TensorFlow: Large-Scale Machine Learning on Heterogeneous Distributed Systems”.
487 In: (Mar. 2016). arXiv: 1603.04467 [cs.DC].

488 [43] Kieran R Campbell and Christopher Yau. “Probabilistic modeling of bifurcations in single-cell gene ex-
489 pression data using a Bayesian mixture of factor analyzers”. In: *Wellcome Open Research* 2 (2017).

490 [44] Peter V Kharchenko, Lev Silberstein, and David T Scadden. “Bayesian approach to single-cell differential
491 expression analysis.” In: *Nature methods* 11.7 (July 2014), pp. 740–2. ISSN: 1548-7105. DOI: 10.1038/nmeth.2967. URL: <http://www.ncbi.nlm.nih.gov/pubmed/24836921>.

493 [45] Michael E Tipping and Christopher M Bishop. “Probabilistic principal component analysis”. In: *Journal of
494 the Royal Statistical Society: Series B (Statistical Methodology)* 61.3 (1999), pp. 611–622.

495 [46] Matthew D Homan and Andrew Gelman. “The no-U-turn sampler: Adaptively setting path lengths in
496 Hamiltonian Monte Carlo”. In: *The Journal of Machine Learning Research* 15.1 (2014), pp. 1593–1623.

497 [47] Bob Carpenter et al. “Stan: a probabilistic programming language”. In: *Journal of Statistical Software*
498 (2015).